Supplementary Material

1.1 Supplementary Figures

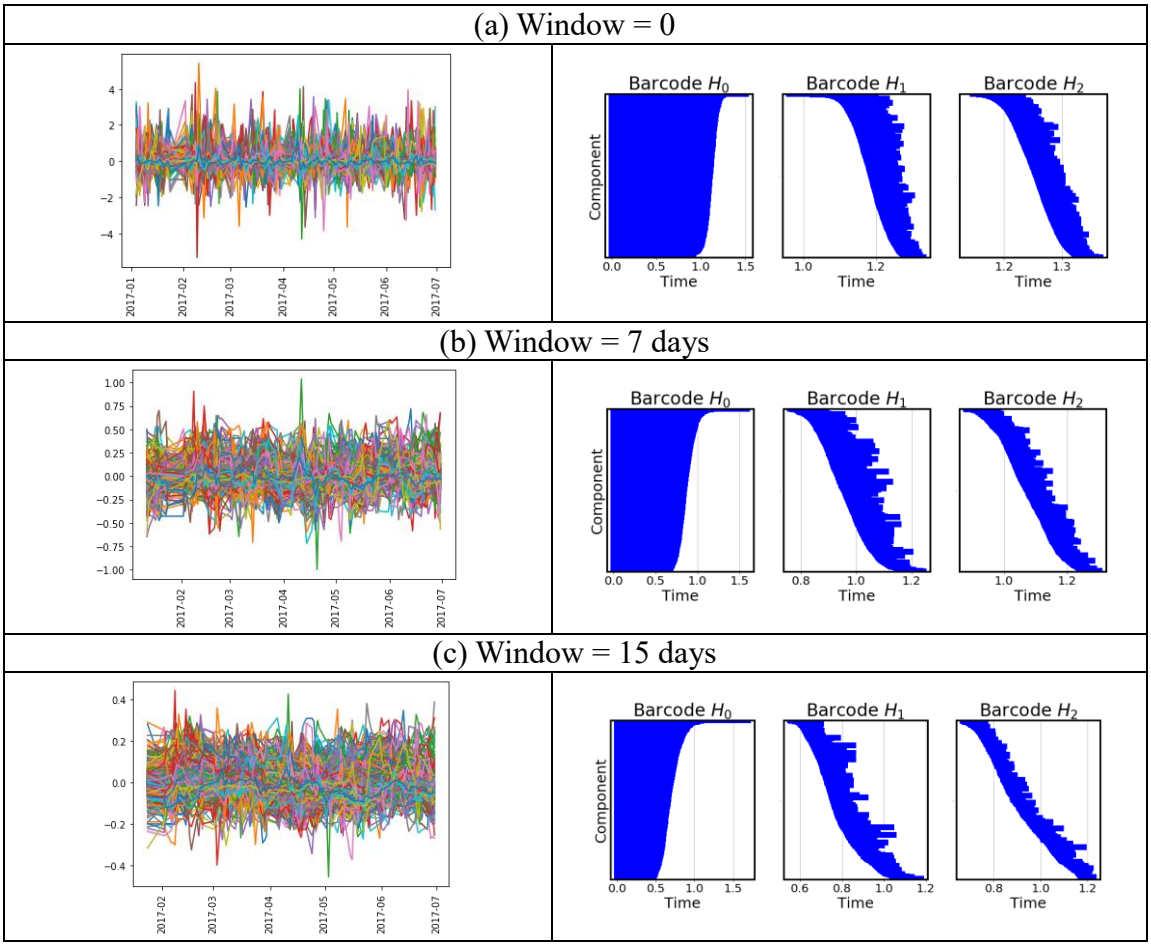

Supplementary Figure S1. We demonstrate how the time series shape changes with different smoothing window sizes. (a) No smoothing on the time series data was affected, (b) a smoothing window size of 7 days was affected, and (c) a smoothing window size of 15 days was affected. For (b), we still found some spikes which will affect the quality of our analysis. Hence, we used a smoothing window size of 15 days as a compromise, which is not too long that starts to lose its quantitative features but also can remove as many spikes as possible.

(a) Two Spheres not overlapped

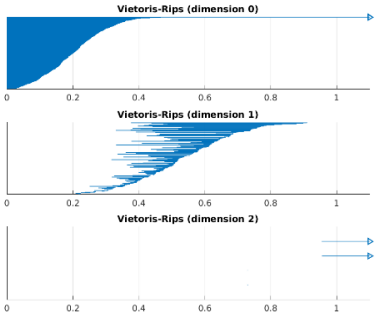

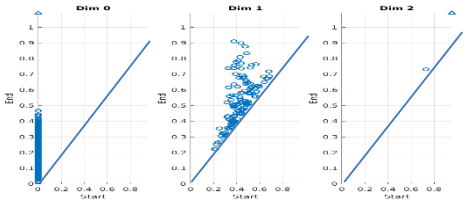

(b) Two spheres touch

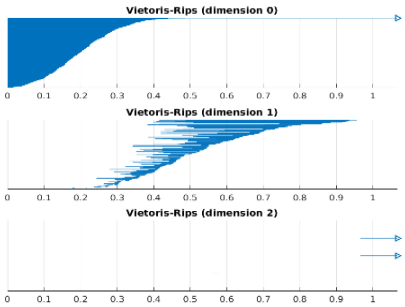

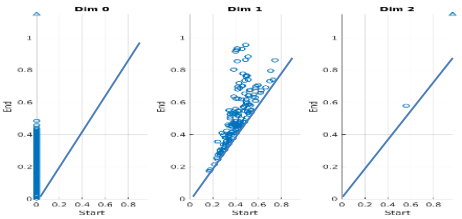

(c) Two spheres overlap

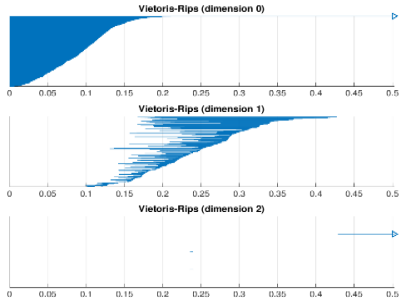

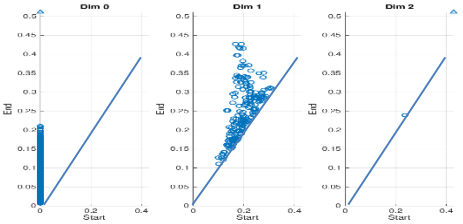

(d) One Sphere

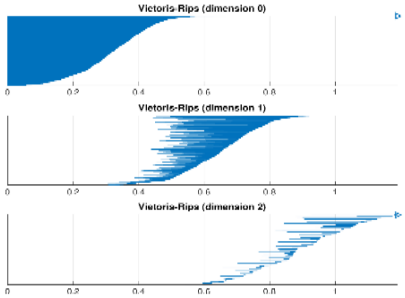

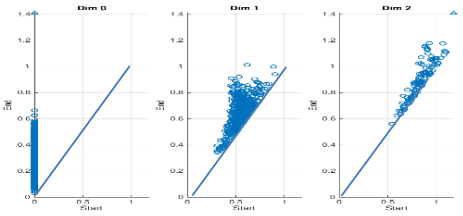

(e) Torus (ρ = 3)

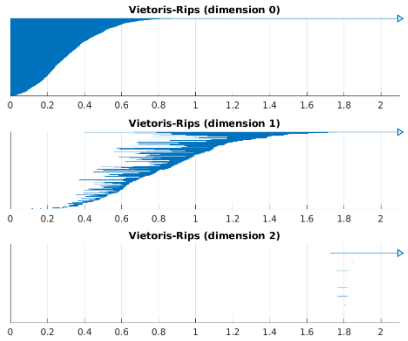

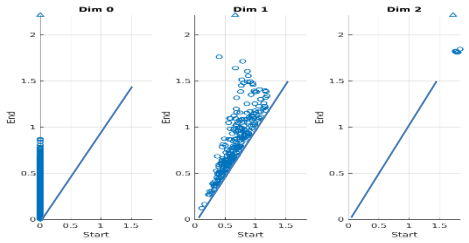

(f) Horn torus

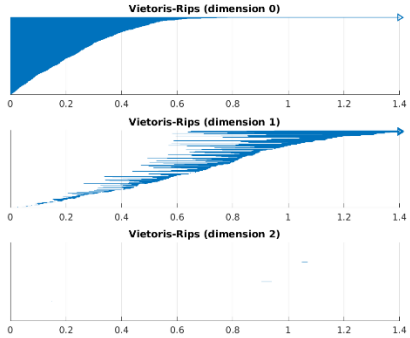

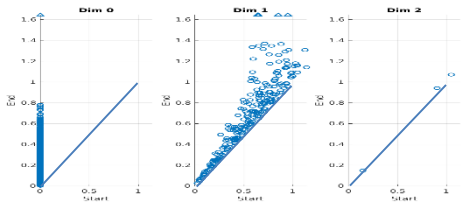

(g) Spindle torus

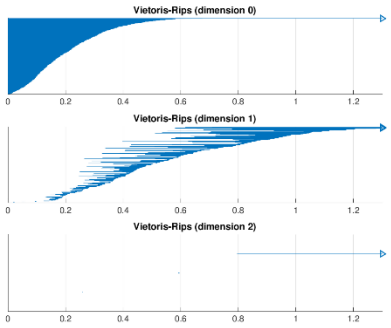

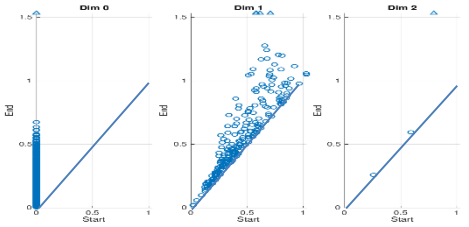

(h) Ellipsoid (a = 5)

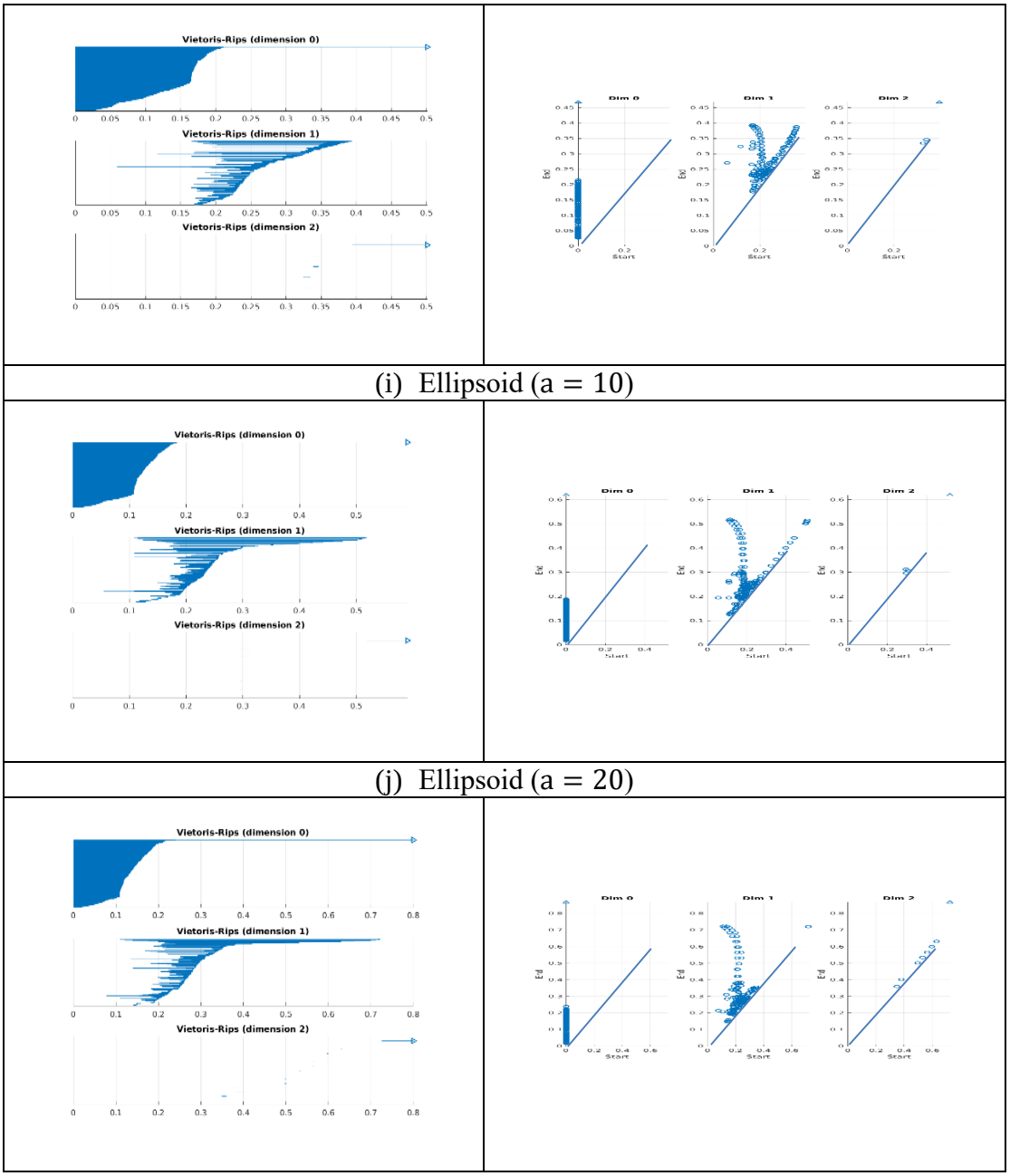

(i) Ellipsoid (a = 10)

(j) Ellipsoid (a = 20)

Supplementary Figure S2. Barcodes, and persistent diagrams up to 2-dim for the toy models introduced in section 3 in the main text. Results are computed using Javaplex software. (a) − (d) correspond to case 1 in the toy models, which is the topological deformation of spheres. (e) − (g) correspond to case 2, i.e. the topological deformations of toruses, and (h) − (j) correspond to topological deformation of ellipsoids (a is one of the axes, and we fix the length of the other two axes one). The arrows in barcodes and persistent diagrams imply an open right boundary for the barcodes. In case one when two spheres are separated, we saw two most persistent bars (mpbs), implying $\beta_0 = 2$; when two spheres merged into one, we see the number of mpb reduce to one, whereas in H_2, the number of mpbs changes from two to one. In the second case subfigure (e) we examine a normal torus (which has the radius of the tube as two, and the distance from the center of the tube to the center of the torus as $\rho = 3$), we see one mpb in 0-dim, and 2-dim, and two mpbs in 1-dim, which correspond

well with mathematical predictions; we then compared the horn torus, and spindle torus with the normal torus and found that the number of mpbs and the length of other bars are all different. The final case is ellipsoids with deformations. We see that the number of mpbs is the same in all three cases, but for other bars, they show some slight differences.

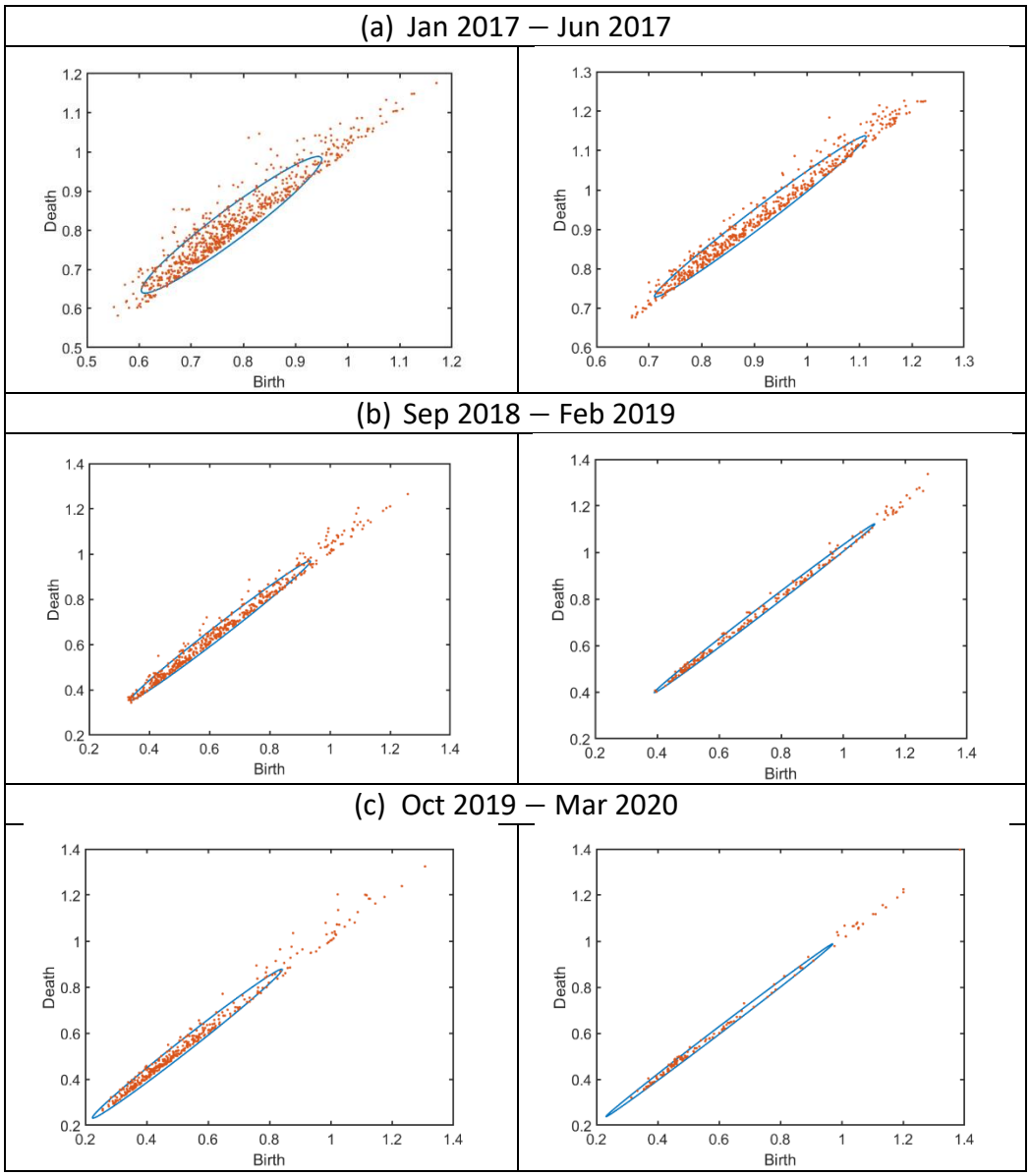

Supplementary Figure S3. We quantified the persistence-weakening phenomena by measuring the principal axis of a covariance error ellipse. Suppose we have data points $\{(x_i, y_i)\}_{i=1}^{N}$. We can construct the covariance matrix $\Gamma = \begin{bmatrix} \gamma_{xx} & \gamma_{xy} \\ \gamma_{xy} & \gamma_{yy} \end{bmatrix}$, where $\gamma_{xx} = \langle (x - \langle x \rangle)^2 \rangle$, $\gamma_{yy} = \langle (y - \langle y \rangle)^2 \rangle$, $\gamma_{xy} = \langle (x - \langle x \rangle)(y - \langle y \rangle) \rangle$. Here we set a confidence level of 68.3% (representing one standard deviation) and plotted the principal variances of the resultant covariance error ellipse (blue color). We selected three

periods in TAIEX, namely (a) a normal market state from Jan 2017 to Jun 2017, (b) a mini-crash from Sep 2018 to Feb 2019, and (c) the COVID-19 crash from Oct 2019 to Mar 2020.

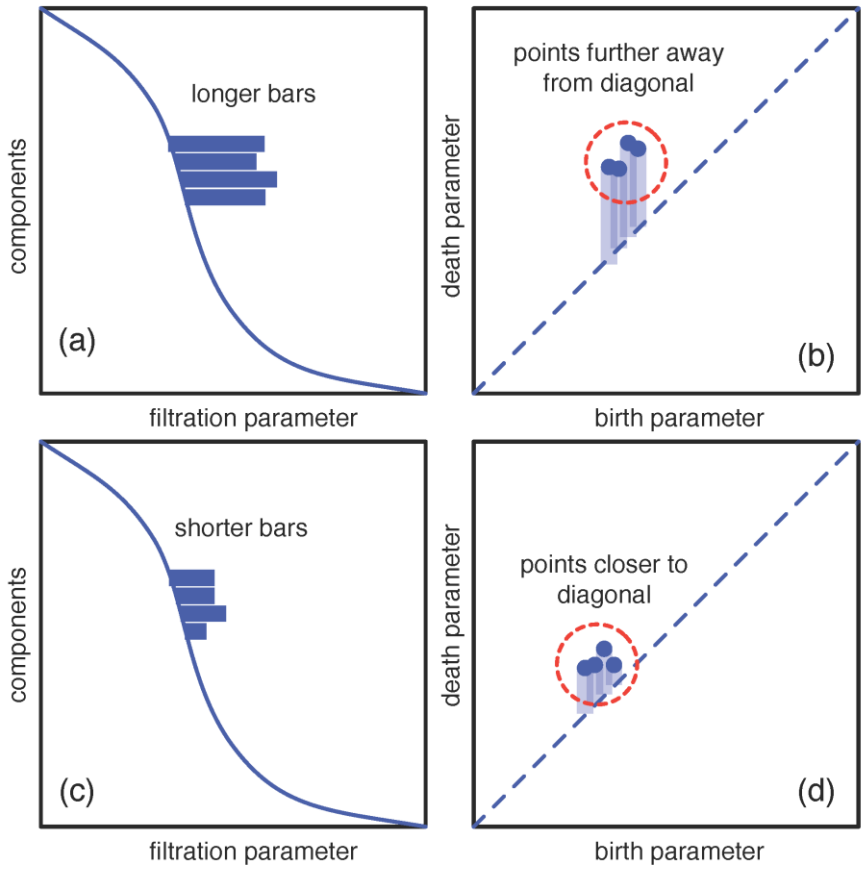

Supplementary Figure S4. Here we show a schematic diagram depicting the persistent weakening phenomena discovered in TAIEX. In (a), we show part of a typical barcode commonly seen in a normal market phase. We show how four bars in the barcode can be converted to the dots in (b) the corresponding persistent diagram, by first rotating each bar 90° counter-clockwise. We then locate the birth time of each bar on the diagonal dashed line, and then follow the rotated bar vertically upwards until it reaches the death time of the bar. At this point, we add a dot, before removing the rotated bar. In (c) and (d), we show the barcode and persistent diagram during a market crash. Because of persistence weakening, the length of the four bars in (c) now significantly shorter, which implies weaker persistence of the bars. We repeat the same procedure of converting bars to rotated bars in the persistent diagram as in the case of a normal market, and we found that these shorter bars lead to dots that are closer to the diagonal line in (d). We recommend readers to refer to both the barcodes and persistent diagrams to detect the persistent weakening episode.